Aerosol and Air Quality Research, 14: 64–73, 2014

ISSN: 1680-8584 print / 2071-1409 online
doi: 10.4209/aaqr.2013.04.0113

Particle Deposition in Respiratory Tracts of School-Aged Children

Regan F. Patterson[1], Qunfang Zhang[2], Mei Zheng[3], Yifang Zhu[2*]

[1] *Department of Chemical and Biomolecular Engineering, University of California, Los Angeles, 405 Hilgard Ave, Los Angeles, CA 90095, USA*
[2] *Department of Environmental Health Sciences, Fielding School of Public Health 51-295 CHS, University of California, Los Angeles, 650 Charles Young Drive South, Los Angeles, CA 90095, USA*
[3] *State Key Joint Laboratory of Environment Simulation and Pollution Control, College of Environmental Sciences and Engineering, Peking University, Beijing 100871, China*

ABSTRACT

Exposure to ultrafine particles poses a potential health risk to school children. While many studies have focused on measuring ultrafine particle (UFP) concentrations in environments where children are at risk of high exposure, few studies have examined the particle deposition in the respiratory tract of children. This study aims to examine the particle deposition in the respiratory tract of school children in different microenvironments. UFP size distribution data were collected in residential homes, school buses, school classrooms, and from school outdoor air in both rural and urban areas of South Texas. The size distribution data were input to the Multiple Path Particle Dosimetry model to calculate regional and total particle deposition fraction. A 24-hour-school-day exposure was simulated by adding the time children spend in each microenvironment. The maximum pulmonary deposition fraction occurs at a diameter ranging from 18 to 40 nm, depending on condition. Age mostly affected the pulmonary region and the total lung deposition with the highest deposition fraction observed for younger children. In addition, comparison of size-dependent regional deposition and particle concentration establishes an accurate depiction of children's exposure and dose profiles. While children only spend 4% of the day in the home source environment, that environment may account for up to 77% of total daily dose intake. Higher deposition fraction occurs at smaller particle size. Younger children show increased levels of particle deposition than older children. Exposure period does not correlate to daily percentage of dose intake. This research can be used to assess children's accumulative exposure to UFPs.

Keywords: Lung deposition; Ultrafine particles; Microenvironments; Exposure; Dose.

INTRODUCTION

Many adverse health effects are associated with particulate matter (PM), such as respiratory and cardiovascular problems (Donaldson and Stone, 2003). It is argued that adverse effects depend on the physicochemical characteristics of PM, such as size, chemical composition, surface structure, shape, and aggregation (Oberdörster *et al.*, 2005a). Ultrafine particles (UFPs, diameter < 100 nm), which dominate particle number concentrations, have been shown to have increased toxicity relative to fine particles of the same material per given mass (Oberdörster, 2000). One epidemiological study showed that decrease in lung function is more closely related to UFP number than to fine particle ($PM_{2.5}$) mass (Peters *et al.*, 1997). The mechanism for toxic effects of UFPs is not fully understood. Lung deposition efficiency may be an important factor (Asgharian and Price, 2007). UFPs are expected to penetrate deep into the lung due to their small size (Oberdörster *et al.*, 2005a). Additionally, UFPs play an important role as carriers of mutagens into the lung (Kawanaka *et al.*, 2011). Thus, it is critical to have detailed assessment of lung deposition in order to determine toxicity and elucidate potential health risks associated with UFPs.

Dosimetry models have been developed to predict lung deposition of UFPs. Included among these are semi-empirical compartmental models (e.g., (ICRP, 1994)), single-path models (e.g., (Choi and Kim, 2007)), multiple-path models (e.g., (Asgharian *et al.*, 2001; Hofmann *et al.*, 2003)), and computational fluid dynamic (CFD) models (Yu *et al.*, 1996; Yu *et al.*, 1998; Hofmann *et al.*, 2003; Shi *et al.*, 2004; Zhang and Kleinstreuer, 2004; Zhang *et al.*, 2005; Zamankhan *et al.*, 2006; Shi *et al.*, 2008; Xi and Longest, 2008). In this study, the Multiple-Path Particle Dosimetry (MPPD) model is used because it simulates both regional and total lung

* Corresponding author.
Tel.: 1-310-825-4324; Fax: 1-310-794-2106
E-mail address: yifang@ucla.edu

deposition. This is necessary because the occurrence of lung diseases depends on the amount of deposit in the whole or specific regions of the lungs, and the regional pattern of deposition of inhaled particles is often a determinant of pathogenic potential (Balásházy *et al.*, 2003). For UFPs, the MPPD model includes axial diffusion and dispersion by axial streaming and, the transport and deposition mechanisms specific to UFPs (Asgharian and Price, 2007). It also incorporates realistic, asymmetric lung structures and a detailed description of the human airway morphology (Hofmann, 2011). In addition, the MPPD model incorporates individual breathing parameters such as functional residual capacity, upper respiratory tract volume, tidal volume, and breathing frequency. Agreement between model predictions and experimental measurements corroborate the validity of this model (Asgharian and Price, 2007). All combined, the MPPD model is a realistic deposition model that will give an accurate prediction of UFP deposition.

Deposition studies have typically focused on adult subjects, little is known about particle deposition in the respiratory tract of children. However, children's high inhalation rates and lung surface area per body weight make them especially susceptible to UFPs (Thurston, 2000). There is a need to evaluate UFP deposition in the important subpopulation of children.

Knowledge of children's lung deposition will establish the relationship between exposure and dose and is necessary to better understand adverse health effects associated with UFPs. Many studies have focused on microenvironment UFP concentrations to which children are frequently exposed, such as on a school bus and in a classroom. Previous studies show that children are particularly exposed to high levels of air pollutants aboard school buses (Sabin *et al.*, 2004; Adar *et al.*, 2008) and near roadways (Zhu *et al.*, 2009). Onboard levels are as much as 2–10 times larger than ambient concentrations (Adar *et al.*, 2008). UFP concentrations are high near a roadway, exponentially decreasing downwind with distance from a roadway (Hitchins *et al.*, 2000; Zhu *et al.*, 2002a, b; Zhu *et al.*, 2009). Although such studies have shown microenvironments with high levels of UFPs, there are no studies detailing whether dose levels reflect the level of exposure.

The current study aims to simulate and assess the deposition of particles in the lung airways of school-aged children in order to obtain an accurate depiction of children's exposure and dose profiles. Using the MPPD model of deposition, along with direct measurement of UFP concentration in the residential home, school bus, classroom, and outdoor air, deposition was modeled through a three-part investigation: (1) the effect of age, breathing pattern, and activity level on particle deposition fraction; (2) the effects of different microenvironments on deposition; and (3) which microenvironment accounts for the greatest percentage of exposure during a school day.

METHODS

Data Sources

The collections of UFP size distribution data in different environments were described in details elsewhere (Zhang *et al.*, 2010; Zhang and Zhu, 2010, 2011). Briefly, UFP size distribution in the size range from 7.6 to 98.2 nm were measured by a Scanning Mobility Particle Sizer (SMPS 3936, TSI Inc., St. Paul., MN) in the following microenvironments: residential home, school buses, school classrooms, and school outdoor air. The data collected in a one-story, 140-m^2 single family house was selected to represent the typical UFP size distributions in residential indoor environments (Zhang *et al.*, 2010). UFP number concentrations in the house were measured for six days in July 2008. Cooking is a common indoor source of UFPs with high emission rate. Thus, a 1-hour cooking episode observed with the highest level of UFPs during six study days was selected to represent the high exposure scenario when children stay at home. Such 1-hour episode included both cooking and dining time to cover high exposures during dining time when UFP level was still high. For comparison, a 1-hour non-cooking episode in early morning, when no indoor source of UFPs was observed, was selected to represent the low exposure scenario in residential indoor environments.

Exposure data when riding school buses were collected in two diesel-powered school buses, one 1990 model year and one 2006 model year (Zhang and Zhu, 2010). UFP size distribution data were collected inside both buses from March 18 through 20, 2008. Air sampling was conducted in the rear of the school bus cabins with children on board to reflect actual exposure for children. To cover a wide range of exposure scenarios in school buses, the data collected under different conditions were utilized, including: (1) when air conditioning (AC) systems were either turned on or off during driving on regular routes, and (2) when the engines were either turned on or off during waiting in school parking lot to pick up or drop off children.

For the exposure in school classrooms, both indoor and outdoor UFP size distributions were collected in five school sites in South Texas between February 2009 and February 2010 (Zhang and Zhu, 2011). The highest UFP level was detected in a library with two vented gas fan heaters; therefore the measurement in this room was used as a representative of high exposure in school indoor environments. For comparison, the measurement in a classroom at the same school site with no indoor source of UFPs observed was selected to represent low exposure scenario in school indoor environments. Since children spend a non-negligible fraction of time outdoors in schools and their activity levels are usually high outdoors, the exposure to outdoor air is also considered for total exposure assessment. The outdoor measurements for two school sites, one in rural residential area with low traffic and one in densely populated urban area near a major urban road with heavy traffic, were employed as two exposure extremes.

The low exposure and high exposure settings in each microenvironment were then used to construct two hypothetical 24-hour-school-day exposure extremes. The high extreme incorporates environments with high exposure and sources, whereas the low extreme incorporates those environments with low exposure and no sources. These scenarios are employed in order to estimate the range of

exposure-dose profiles.

Modeling Procedure

The particle size distribution data from each microenvironment were utilized in the MPPD model as input parameters. The MPPD model requires aerosol concentration to be input as a mass. To convert particle number size distribution data to mass concentration, the particle volume was first computed under the assumption of spherical shape. This volume was then multiplied by the commonly used density of 1.2 g/cm^3 (Liu *et al.*, 2009) to calculate mass per particle. That value was multiplied by the number concentration to achieve mass concentration. The particle diameter and mass concentration were then input into the model.

The MPPD models the respiratory tract as three regions: head airway region, tracheobronchial region, and pulmonary region. Deposition calculations of UFPs are performed in age-specific morphometric models of the human lung based on Mortensen *et al.* (1983a, b, 1989). To model school-aged children, the lung geometries for ages 8, 9, 14, and 18 were chosen. These were the four ages available in the MPPD model that were within the typical age range of school children in the US - age 4 to age 18. The lung and breathing parameters for each age are shown in Table 1. These values are applicable at rest (no physical exertion). As one of the goals of this study was to measure the effect of activity on particle deposition fraction, it was important to calculate breathing parameters not just at rest, but also for other levels of physical exertion. The designated activity levels chosen to examine were rest, light activity, and heavy activity. These correspond to sitting, walking, and jogging, respectively. Physical activity influences tidal volume and breathing frequency according to the following scaling rules: tidal volume for light and heavy activity is increased by a factor of 2 and 3, respectively, compared to rest; breathing frequency for light and heavy activity is increased by a factor of 1.5 and 2, respectively (Hofmann, 1982). In addition, the breathing patterns commonly associated with each level of physical exertion were considered: nasal breathing for rest and light activity, oronasal breathing for heavy activity. Different breathing patterns were also independently considered by comparing nasal and oral breathing. The regional and total deposition of UFPs were quantified by the MPPD model in terms of the deposition fraction during one breathing cycle in each region of the respiratory tract.

Total deposit was determined by multiplying the deposition fraction by the number concentration. In order to capture a dose profile of a 24-hour school day, total number of deposited particles was multiplied by the minute ventilation (tidal volume multiplied by breathing frequency) and time spent in each environment. During the 24 hour exposure period, UFP deposit in each microenvironment was defined as the sum of the deposited particles with size between 7.6 and 98.2 nm, as measured by the SMPS. Table 2 shows the hypothetical breakdown of time that a representative 8-year-old child spent in each microenvironment, along with activity level and breathing pattern. These times were based on observations and literature data (Abt *et al.*, 2000; Hofferth and Sandberg, 2001; Zhang and Zhu, 2010, 2011). The total time spent indoors is in agreement with reports that children spend 80–90% of their time indoors (U.S. EPA, 2002). The hypothetically constructed scenarios represent high and low exposure extremes.

RESULTS AND DISCUSSION

Summary of Measured UFP Concentrations

Table 3 presents a summary of the average UFP concentrations, calculated for each particle size bin between 7.6 and 98.2 nm, in each microenvironment. Average UFP concentrations for home with no indoor source and for home with a cooking source were 160 particles/cm^3 and 140,000 particles/cm^3, respectively. Average UFP concentrations for the school bus stationary with windows open and engine off and for the idling bus with windows open were 2,900 particles/cm^3 and 41,000 particles/cm^3, respectively. Average UFP concentrations for the school bus running with windows closed/no AC and for the school bus running with windows closed/AC on were 11,000 particles/cm^3 and 1,200 particles/cm^3. Average UFP concentrations for the classroom with indoor source (heater) and for the classroom with no indoor source were 2,900 particles/cm^3 and 260 particles/cm^3. Average UFP concentrations for school outdoor rural area and for school outdoor near roadway were 810 particles/cm^3 and 3,000 particles/cm^3, respectively. The environment with the highest children exposure was home during cooking, followed by inside a bus idling and inside a bus running with no AC.

Table 1. Breathing parameters at rest (no physical exertion) for each age category. For all ages modeled (8, 9, 14, and 18) four components of breathing are incorporated into the model. In order to model light activity (walking) or heavy activity (jogging), the breathing parameters listed would be multiplied as follows: 1) tidal volume for light and heavy activity is multiplied by a factor of 2 and 3, respectively; 2) breathing frequency for light and heavy activity is increased by a factor of 1.5 and 2, respectively. Upper respiratory tract and tidal volumes remain identical as those depend only on age and not activity level.

Age	Functional Residual Capacity (mL)	Upper Respiratory Tract Volume (mL)	Breathing Frequency (min^{-1})	Tidal Volume (mL)
8	501.3	21.0	17	278.2
9	683.0	22.4	17	295.8
14	987.6	30.6	16	388.1
18	1159.4	37.4	15	446.7

Table 2. Hypothetically constructed 24-hour school day for an 8-year-old child with time spent in each microenvironment. The activity level (rest, light, or heavy) along with the breathing pattern (nasal or oronasal) are included for each microenvironment.

Activity	Activity Level	Breathing Pattern	Extreme Low (hr)	Extreme High (hr)
Home Source	Light	Nasal	0	1
Home No Source				
Sleep	Rest	Nasal	10	10
Awake	Light	Nasal	6	5
Bus Stationary				
Engine Off	Light	Nasal	0.5	0
Engine On	Light	Nasal	0	0.5
Bus Running				
AC	Rest	Nasal	1.5	0
No AC	Rest	Nasal	0	1.5
Classroom				
No Heater	Rest	Nasal	5.5	0
Heater	Rest	Nasal	0	5.5
School Outdoor				
Rural Area	Heavy	Oronasal	0.5	0
Near Roadway	Heavy	Oronasal	0	0.5

Table 3. Summary of UFP concentrations in each microenvironment.

Environment	Average Number Concentration (particles/cm^3)
Home Source	140,000 (110,000) *
Home No Source	160 (90)
Bus Stationary – Engine Off	2,900 (1,400)
Bus Stationary – Engine On	41,000 (35,000)
Bus Running – No AC	11,000 (9,800)
Bus Running – AC	1,200 (700)
Classroom – Heater	2,900 (2,700)
Classroom – No Heater	260 (140)
School Outdoor – Rural Area	810 (290)
School Outdoor – Near Roadway	3,000 (2,700)

* Standard deviations are given in parentheses.

Factors Affecting Lung Deposition

Particle Diameter

For each particle size between 7.6 and 98.2 nm, the deposition fraction in each region of the respiratory tract was calculated. The deposition fraction for each diameter was plotted for the varying conditions: age, breathing pattern, and activity level. Fig. 1 depicts the typical deposition fraction for one of these conditions - that of an 8-year old child, taken at a resting level of physical exertion with nasal breathing. The patterns shown in Fig. 1 are representative of the trends in the deposition curves observed for all conditions. The specific deposition fractions differ when considering different breathing patterns and physical levels of exertion. If Fig. 1 simulated oral breathing, there would be a lower total lung deposition fraction. If Fig. 1 simulated light activity or heavy activity, there would be lower total lung deposition fraction for particles greater than 30 nm and for all particles, respectively. Though the deposition fractions may differ, the same deposition trends are observed for all conditions.

The highest total deposition fraction occurs for the smallest particle size. Total lung deposition decreases with an increase in particle size within the UFP size range. This is in agreement with diffusion theory, which states that there is increased total capture efficiency of the smaller UFPs in the respiratory tract. Higher deposition fraction and smaller size increased their chance to penetrate deep into the lung with more mutagens, implicating higher health risk associated with the smaller UFPs.

The total lung deposition curve is a result of the regional deposition patterns. It is seen that the regional deposition patterns of UFPs are non-uniform. In particular, while the deposition curves decrease with increasing diameter in both the head airway and tracheobronchial regions, the pulmonary deposition is parabolic in shape. The parabolic shape of pulmonary deposition is consistent with the deposition mechanisms. The peak in pulmonary deposition is due to central airway and tracheobronchial filtering effects (Asgharian and Price, 2007). The diameter at which peak deposition occurs varies among age, breathing pattern, and activity level. The maximum pulmonary deposition fraction occurs at a diameter ranging from 18 to 40 nm, depending on condition. UFPs with a diameter within the peak pulmonary deposition range are a health concern. Once in the pulmonary region, UFPs may penetrate lung tissues and translocate to extrapulmonary sites and reach target organs by different transfer routes and mechanisms (Oberdörster *et al.*, 2005b). Translocation to secondary target organs, such as the cardiovascular system, liver, spleen, bone marrow, central nervous system, and endocrine organs, may induce direct adverse responses (Oberdörster *et al.*, 2005a).

The trends observed in deposition fraction are fixed. To compute the total particle deposition in each region of the respiratory tract, the deposition fraction is multiplied by the number concentration. Thus, the concentration data from each environment are multiplied by the same

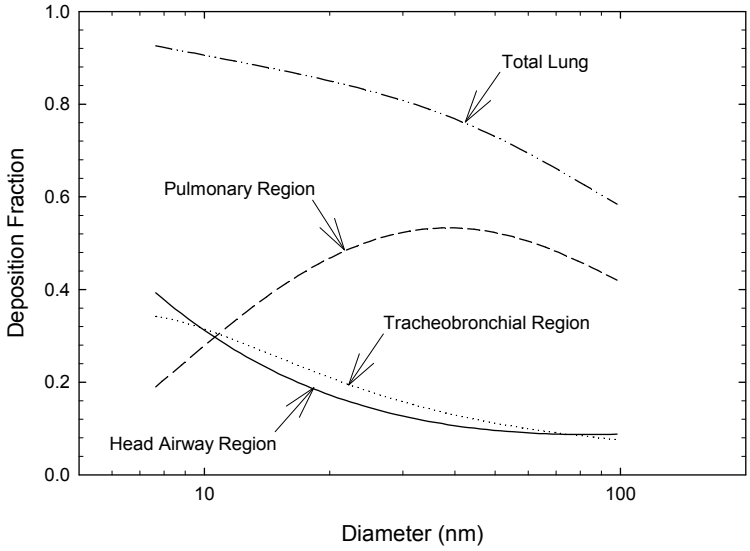

Fig. 1. Typical plot for regional deposition fraction of inhaled particles as a function of particle size. The deposition fraction in this figure is simulated for an 8-yr old under nasal breathing and resting conditions.

fractions. This suggests that the environments with higher exposure lead to higher dose. The environments with the greatest UFP number concentration are the home cooking environment, followed by the school bus stationary with windows open/engine on and then school bus running with windows closed/no AC. Thus, it is these environments that are of particular health concern. This analysis is critical to refine assessment of childhood UFP exposures.

Age

Fig. 2 shows the age-dependent changes in deposition fraction to different regions of the respiratory tract. Predicted head airway and tracheobronchial deposition patterns were similar among the different ages for each particle size. In the head airway and tracheobronchial regions, UFPs are deposited by convective Brownian diffusion. Although airways grow in length and diameter as age progresses (Reid, 1977), Fig. 2 suggests that the mechanism of UFP deposition in these airways was not strongly affected by the size of the airways. Age mostly affected the pulmonary region and the total lung deposition. Deposition in the pulmonary region results from Brownian motion and gravitational settling. After the age of two, there is little or no increase in total alveolar number, but there is an increase in linear dimension and in alveolar volume until adulthood (Thurlbeck. 1982). Thus, UFPs are likely exhaled from larger alveoli due to a greater settling distance resulting from larger airway dimension. This may explain the smaller deposition fraction in pulmonary region for children at age 18 compared to those at age 8. The results in Fig. 2 show that age-dependency is not homogeneous throughout the entire respiratory tract, but varies regionally. In regions where significant difference exists, the amount of difference is dependent on particle size.

Total lung deposition fraction is the highest for children aged 8 and decreases with age at each particle size. As shown in Fig. 2, the pulmonary region is the region affected mostly by age. It is the higher deposition fraction for younger children in this region that results in higher total lung deposit. The observed predictions of particle deposition indicate that the lungs of younger children may have an increased dose of UFPs, and therefore an increased potential health risk from exposure to UFPs.

Microenvironments

Fig. 3 shows number concentration data measured in each microenvironment. The mode for each UFP size distribution is observed by visual inspection of the graph. School bus stationary with engine on, school bus running with no AC, and classroom with a heater have size distributions showing a mode in the size range 10–40 nm. This size range is similar to the size range where maximum pulmonary deposition fraction occurs. This mode is shifted to a larger particle size range for the home source environment. A mode was not clearly observed for the other microenvironments.

Fig. 4 displays the relationship between exposure in a classroom with a source and the resulting deposition in each region of the respiratory tract. The trends observed in Fig. 1 are repeated in Fig. 4. The total lung deposition curve is identical in shape to that of the concentration curve. However, as particle diameter increases, the amount of difference between particle concentration and deposition increases. This is in agreement with the downward slope observed in total lung deposition fraction shown in Fig. 1. In addition, as particle diameter increases, the amount of difference between particle concentration and deposition in both the head airway and the tracheobronchial region increases. This is also in agreement with the downward slope in the deposition fraction of these regions. However, the amount of difference increases at a faster rate for the head airway and tracheobronchial regions as compared to the total lung. This is due to the negative concavity of their slope, as compared to the positive concavity of the total lung. Similar relationships were also observed in other microenvironments.

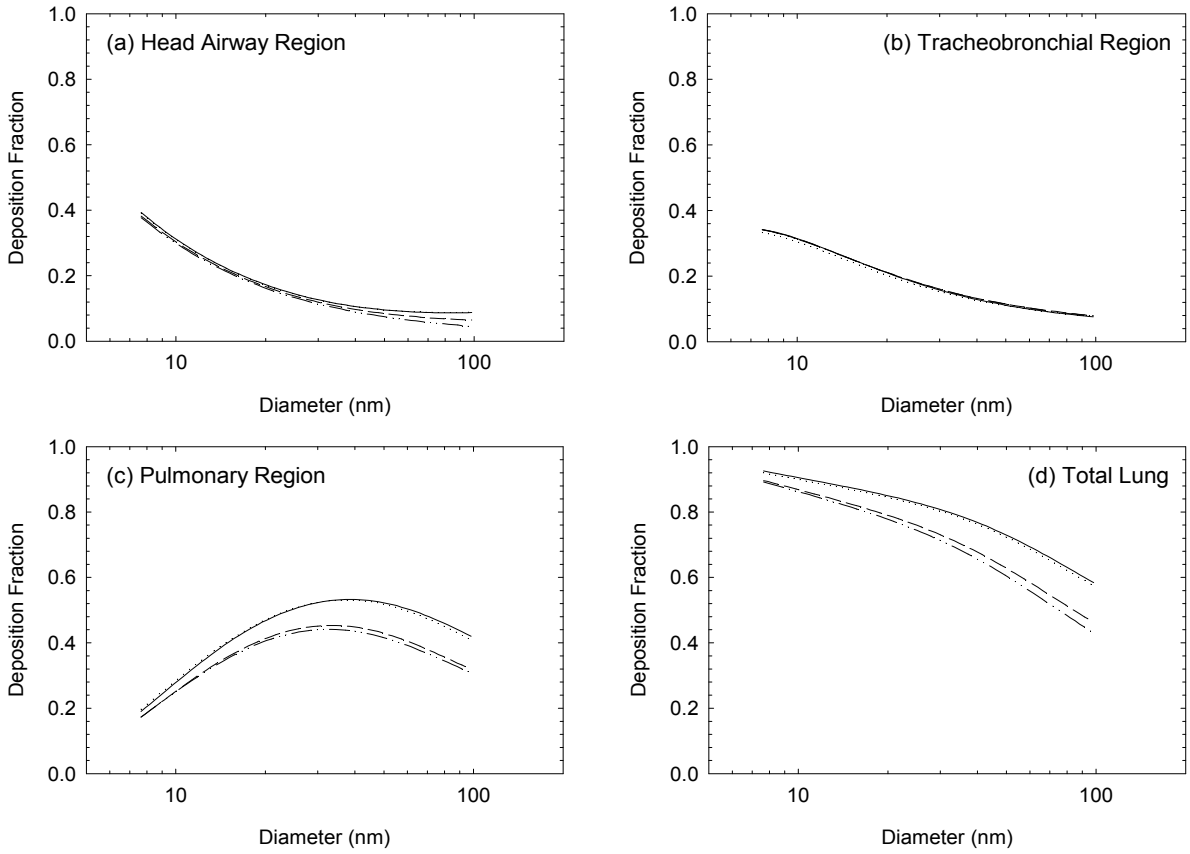

Fig. 2. Impact of age on regional deposition fraction, —— age 8, ------ age 9, – – – – age 14, – ··— ·· age 18. Simulated for the case of nasal breathing and resting activity level.

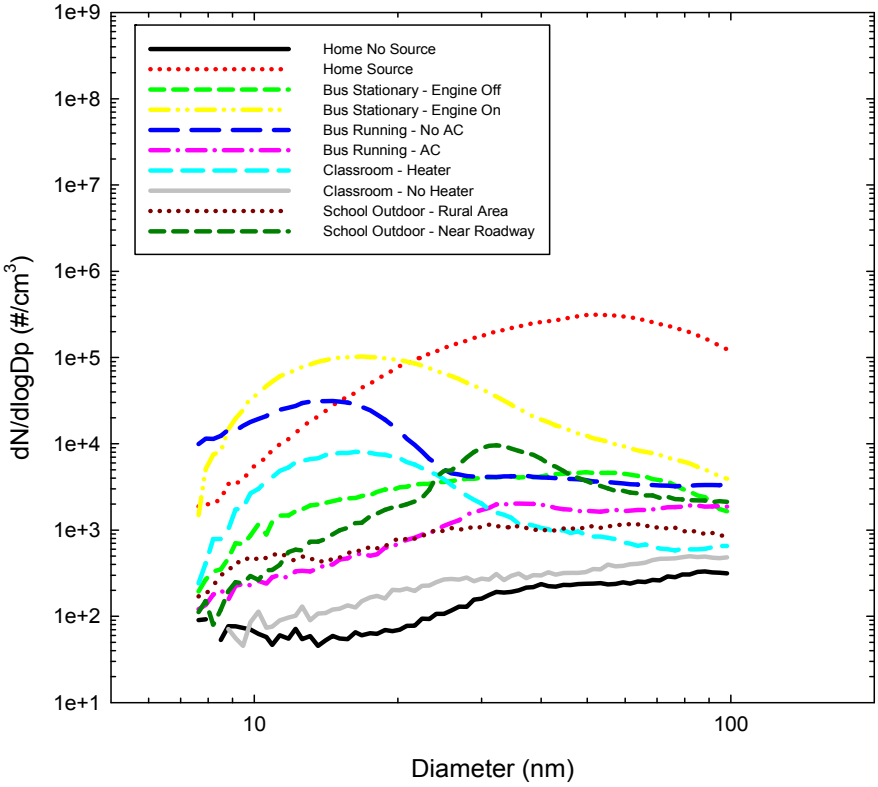

Fig. 3. Ultrafine particle number size distribution in each microenvironment.

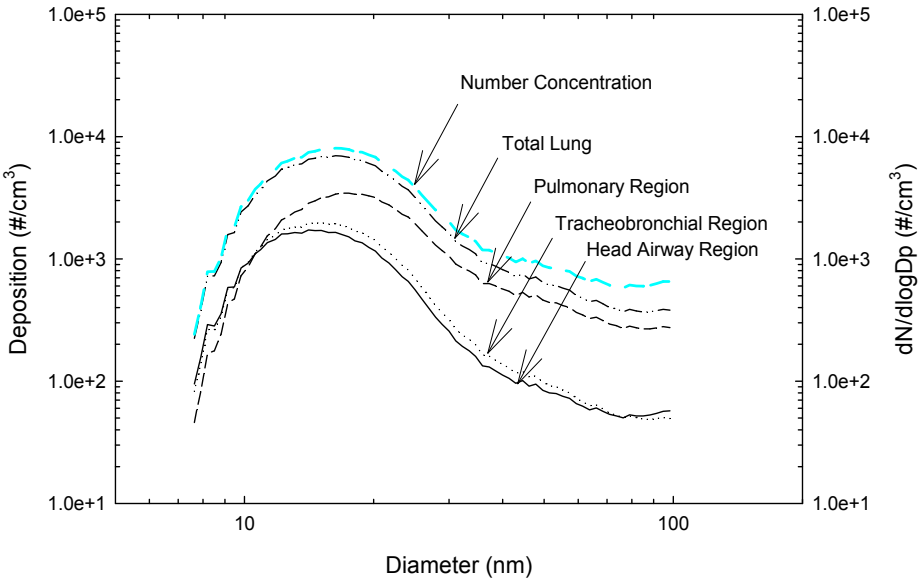

Fig. 4. Relationship between particle concentration and regional deposition as a function of particle size. The blue line represents the classroom particle concentration, while the black lines represent classroom regional deposition.

Simulated Hypothetical 24-hour School Day

Figs. 5 and 6 show the low and high extremes of exposure for an 8-year-old child during a hypothetically constructed 24-hour school day, respectively. Simulation for low exposure incorporated microenvironments with minimum or no pollutant sources. Thus, environments such as the home with no sources and the classroom with no heater were included in computation. For comparison, simulation for high exposure included environments such as the home with source and bus idling. Figs. 5(a) and 6(a) indicate time spent in each environment. The times used for calculation are shown in Table 2. Figs. 5(b) and 6(b) indicate total lung deposition. As indicated in Fig. 6, a child spends only 2% of their day in the school bus cabin while the bus is stationary with the engine on, yet that environment accounts for 14% of total dose.

Figs. 5 and 6 illustrate the range of the exposure-dose profiles. Although the time plots remain similar, the inclusion of UFP sources significantly alters the percentage of daily dose that each environment contributes. For example, while the percentage of daily dose for the home sleeping environment is 10% in the low exposure scenario, the percentage decreases to only 0.3% in the high exposure scenario. In addition, the inclusion of the home with a source significantly alters the percentage of daily dose. While the amount of time spent in the home with a source accounts for only 4% of the 24-hr day, this environment may account for up to 77% of daily dose intake.

Simulation of the hypothetically constructed 24-hour school day shows that the time spent in a microenvironment does not correspond to percentage of daily intake. Factors that account for variation between percentage of time and percentage of daily dose include the amount of time spent in each environment, UFP number concentration, breathing pattern, and activity level. Light and heavy activity levels increase the minute ventilation. This, in turn, increases lung deposition. For instance, the cabin pollutant concentrations and child light activity level led to increased percentage of total lung deposition. In addition, the inclusion of UFP sources significantly altered the percentage of daily dose that each environment contributes. For instance, the change in the percentage of daily dose for the home sleeping environment can be attributed to increased pollutant concentrations of the other environments. Lastly, the inclusion of the home with a source significantly alters the percentage of daily dose. The average UFP concentration for home with a cooking source was 140,000 particles/cm^3. This is an order of magnitude higher than the bus idling concentrations and two orders of magnitude higher than the classroom with a heater. The amount of time spent in the home with a source accounts for only 4% of a 24-hr day. However, high UFP concentration results in this environment having 77% of daily dose intake. Thus, even a small percent of time near high sources is of key importance when assessing health effects. Control of these environments can help reduce exposure.

This study is limited to the microenvironments that we have data from. Thus, the two hypothetically constructed 24-hour school days do not provide a distribution for US children in general. In addition, this study was conducted in South Texas. The results are representative of a rural area, and the pollution levels may be lower than more densely populated areas. However, the method used and knowledge gained from this study may be generalized to children living in other locations.

CONCLUSION

Particle deposition in the respiratory tract of school children aged 8 to 18 years old was computed using the MPPD model. Age, breathing pattern, and activity level impact regional deposition fraction. Higher deposition

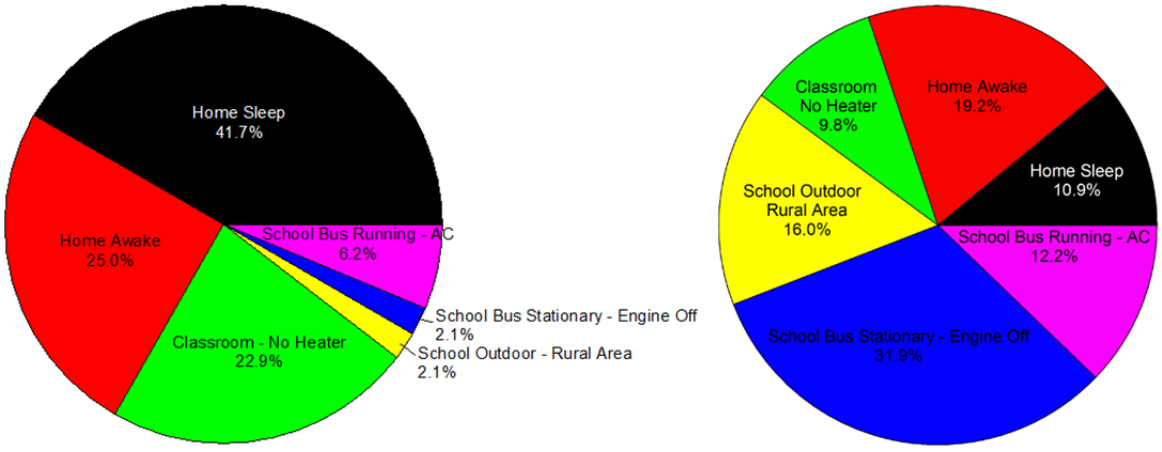

Fig. 5. Simulated hypothetical low exposure scenario with little or no sources. Comparison of (a) percentage of time spent in each environment during a 24-hr school day and (b) percentage of daily dose for an 8-year-old child.

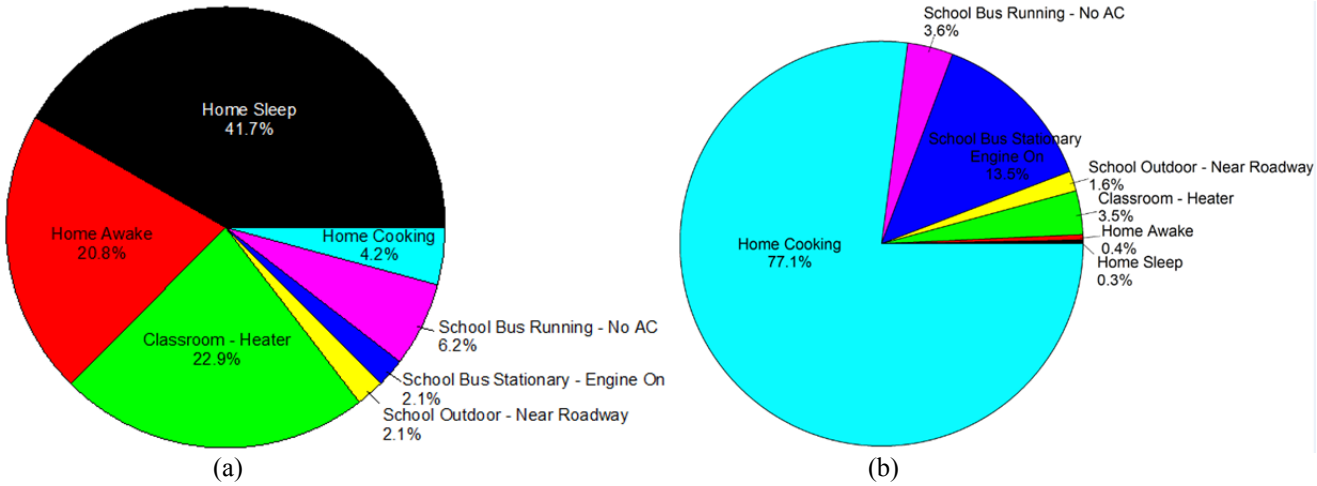

Fig. 6. Simulated hypothetical high exposure scenario with sources. Comparison of (a) percentage of time spent in each environment during a 24-hr school day and (b) percentage of daily dose for an 8-year-old child.

fraction occurs at smaller particle size. In addition, younger children show increased levels of particle deposition than older children.

The total number of particles deposited in an 8-year old child's lung within each microenvironment was evaluated. Comparison of size-dependent regional deposition and particle concentration establishes an accurate depiction of children's exposure and dose profiles. In addition, a 24-hour school day exposure period was simulated with number of hours children spend in each microenvironment. Exposure period does not correlate to daily percentage of dose intake. While children only spend 4% of the day in the home source environment, that environment may account for up to 77% of total daily dose intake. This research can be used to assess children's accumulative exposure to UFPs. Overall, this research is critical to refine assessment on exposure and even has policy implications. For instance, understanding exposure in different microenvironments allows the targeting of key problem environments where high levels of UFPs are expected.

REFERENCES

Abt, E., Suh, H.H., Allen, G. and Koutrakis, P. (2000). Characterization of Indoor Particle Sources: A Study Conducted in the Metropolitan Boston Area. *Environ. Health Perspect.* 108: 35–44.

Adar, S.D., Davey, M., Sullivan, J.R., Compher, M., Szpiro, A. and Sally Liu, L.J. (2008). Predicting Airborne Particle Levels aboard Washington State School Buses. *Atmos. Environ.* 42: 7590–7599.

Asgharian, B., Hofmann, W. and Bergmann, R. (2001). Particle Deposition in a Multiple-path Model of the Human Lung. *Aerosol Sci. Technol.* 34: 332–339.

Asgharian, B. and Price, O.T. (2007). Deposition of Ultrafine (Nano) Particles in the Human Lung. *Inhalation Toxicol.* 19: 1045–1054.

Balásházy, I., Hofmann, W. and Heistracher, T. (2003). Local Particle Deposition Patterns May Play a Key Role in the Development of Lung Cancer. *J. Appl. Physiol.* 94: 1719–1725.

Choi, J.I. and Kim, C.S. (2007). Mathematical Analysis of Particle Deposition in Human Lungs: An Improved Single Path Transport model. *Inhalation Toxicol.* 19: 925–939.

Donaldson, K. and Stone, V. (2003). Current Hypotheses on the Mechanisms of toxicity of Ultrafine Particles: Il Material Particellare Aerodisperso: Proprieta, Misure, Norme ED Effetti Sulla Salute *Ann. Ist. Super. Sanità* 39: 405–410.

Hitchins, J., Morawska, L., Wolff, R. and Gilbert, D. (2000). Concentrations of Submicrometre Particles from Vehicle Emissions near A Major Road. *Atmos. Environ.* 34: 51–59.

Hofferth, S.L. and Sandberg, J.F. (2001). How American Children Spend Their Time. *J. Marriage Fam.* 63: 295–308.

Hofmann, W. (1982). Mathematical Model for the Postnatal Growth of the Human Lung. *Respir. Physiol.* 49: 115–129.

Hofmann, W., Golser, R. and Balásházy, I. (2003). Inspiratory Deposition Efficiency of Ultrafine Particles in a Human Airway Bifurcation Model. *Aerosol Sci. Technol.* 37: 988–994.

Hofmann, W. (2011). Modelling Inhaled Particle Deposition in the Human Lung—A Review. *J. Aerosol Sci.* 42: 693–724.

ICRP (1994). Human Respiratory Tract Model for Radiological Protection. *Ann ICRP* 24: 1–482.

Kawanaka, Y., Matsumoto, E., Sakamoto, K. and Yun, S.J. (2011). Estimation of the Contribution of Ultrafine Particles to Lung Deposition of Particle-bound Mutagens in the Atmosphere. *Sci. Total Environ.* 409: 1033–1038.

Liu, Z.G., Vasys, V.N., Dettmann, M.E., Schauer, J.J., Kittelson, D.B. and Swanson, J. (2009). Comparison of Strategies for the Measurement of Mass Emissions from Diesel Engines Emitting Ultra-low Levels of Particulate Matter. *Aerosol Sci. Technol.* 43: 1142–1152.

Mortensen, J., Schaap, R., Bagley, B., Stout, L., Young, J., Stout, A., Burkart, J. and Baker, C. (1983a). Final Report: A Study of Age Specific Human Respiratory Morphometry. University of Utah Research Institute, UBTL Division, University of Utah, Salt Lake City, UT 01525–01010.

Mortensen, J., Young, J., Stout, L., Stout, A., Bagley, B. and Schaap, R. (1983b). A Numerical Identification System for Airways in the Lung. *Anat. Rec.* 206: 103–114.

Mortensen, J., Stout, L., Bagley, B., Burkart, J., Schaap, R., Crapo, J., Smolko, E., Miller, F., Graham, J. and Hayes, A. (1989). Age Related Morphometric Analysis of Human Lung Casts, In *Extrapolation of Dosimetric Relationships for Inhaled Particles and Gases*, Crapo, J., Smolko, E., Miller, F., Graham, J. and Hayes, A. (Eds.), CA Academic Press, San Diego, p. 59–68.

Oberdörster, G. (2000). Pulmonary Effects of Inhaled Ultrafine Particles. *Int. Arch. Occup. Environ. Health* 74: 1–8.

Oberdörster, G., Maynard, A., Donaldson, K., Castranova, V., Fitzpatrick, J., Ausman, K., Carter, J., Karn, B., Kreyling, W. and Lai, D. (2005a). Principles for Characterizing the Potential Human Health Effects from Exposure to Nanomaterials: Elements of a Screening Strategy. *Part. Fibre Toxicol.* 2: 8.

Oberdörster, G., Oberdörster, E. and Oberdörster, J. (2005b). Nanotoxicology: An Emerging Discipline Evolving from Studies of Ultrafine Particles. *Environ. Health Perspect.* 113: 823.

Peters, A., Wichmann, H.E., Tuch, T., Heinrich, J. and Heyder, J. (1997). Respiratory Effects are Associated with the Number of Ultrafine Particles. *Am. J. Respir. Crit. Care Med.* 155: 1376–1383.

Reid, L. (1977). 1976 Edward B.D. Neuhauser Lecture: The Lung: Growth and Remodeling in Health and Disease *Am. J. Roentgenol.* 129: 777–788.

Sabin, L.D., Behrentz, E., Winer, A.M., Jeong, S., Fitz, D.R., Pankratz, D.V., Colome, S.D. and Fruin, S.A. (2004). Characterizing the Range of children's Air Pollutant Exposure during School Bus Commutes. *J. Exposure Sci. Environ. Epidemiol.* 15: 377–387.

Shi, H., Kleinstreuer, C. and Zhang, Z. (2008). Dilute Suspension Flow with Nanoparticle Deposition in a Representative Nasal Airway Model. *Phys. Fluids* 20: 013301–013323.

Shi, H., Kleinstreuer, C., Zhang, Z. and Kim, C.S. (2004). Nanoparticle Transport and Deposition in Bifurcating Tubes with Different Inlet Conditions. *Phys. Fluids* 16: 2199–2213.

Thurlbeck, W.M. (1982). Postnatal Human Lung Growth. *Thorax* 37: 564–571.

Thurston, G.D. (2000). Particulate Matter and Sulfate: Evaluation of Current California Air Quality Standards with Respect to Protection of Children, Prepared for CARB and OEHHA.

U.S. EPA (2002). Child-specific Exposure Factors Handbook, Washington, D.C., U.S. Environmental Protection Agency.

Xi, J. and Longest, P.W. (2008). Numerical Predictions of Submicrometer Aerosol Deposition in the Nasal Cavity Using a Novel Drift Flux Approach. *Int. J. Heat Mass Transfer* 51: 5562–5577.

Yu, G., Zhang, Z. and Lessmann, R. (1996). Computer Simulation of the Flow Field and Particle Deposition by Diffusion in a 3-d Human Airway Bifurcation. *Aerosol Sci. Technol.* 25: 338–352.

Yu, G., Zhang, Z. and Lessmann, R. (1998). Fluid Flow and Particle Diffusion in the Human upper Respiratory System. *Aerosol Sci. Technol.* 28: 146–158.

Zamankhan, P., Ahmadi, G., Wang, Z., Hopke, P.K., Cheng, Y.S., Su, W.C. and Leonard, D. (2006). Airflow and Deposition of Nano-particles in a Human Nasal Cavity. *Aerosol Sci. Technol.* 40: 463–476.

Zhang, Q. and Zhu, Y. (2010). Measurements of Ultrafine Particles and other Vehicular Pollutants inside School Buses in South Texas. *Atmos. Environ.* 44: 253–261.

Zhang, Q., Gangupomu, R.H., Ramirez, D. and Zhu, Y. (2010). Measurement of Ultrafine Particles and other Air Pollutants Emitted by Cooking Activities. *Int. J. Environ. Res. Public Health* 7: 1744–1759.

Zhang, Q. and Zhu, Y. (2011). Characterizing Ultrafine Particles and other Air Pollutants at Five Schools in South Texas. *Indoor Air* 22: 33–42.

Zhang, Z. and Kleinstreuer, C. (2004). Airflow Structures and Nano-particle Deposition in a Human Upper Airway Model. *J. Comput. Phys.* 198: 178–210.

Zhang, Z., Kleinstreuer, C., Donohue, J.F. and Kim, C.S. (2005). Comparison of Micro- and Nano-size Particle Depositions in a Human Upper Airway model. *J. Aerosol Sci.* 36: 211–233.

Zhu, Y., Hinds, W.C., Kim, S., Shen, S. and Sioutas, C. (2002a). Study of Ultrafine Particles near a Major Highway with Heavy-duty Diesel Traffic. *Atmos. Environ.* 36: 4323–4335.

Zhu, Y., Hinds, W.C., Kim, S. and Sioutas, C. (2002b). Concentration and Size Distribution of Ultrafine Particles near a Major Highway. *J. Air Waste Manage. Assoc.* 52: 1032–1042.

Zhu, Y., Pudota, J., Collins, D., Allen, D., Clements, A., DenBleyker, A., Fraser, M., Jia, Y., McDonald-Buller, E. and Michel, E. (2009). Air Pollutant Concentrations near Three Texas Roadways, Part I: Ultrafine Particles. *Atmos. Environ.* 43: 4513–4522.

Received for review, April 9, 2013
Accepted, September 30, 2013